Fatigue Crack Growth Behavior of a Shielded Metal Arc Welded (SMAW) Structural Steel Weldment

Susil K. Putatunda[1], Abhijit Sengupta[1] and Jack Schaefer[2]

[1]*Department of Materials Science and Engineering, Wayne State University, Detroit, Michigan 48202, USA.*
[2]*Detroit Edison, Detroit, Michigan 48210, USA*

ABSTRACT

Fatigue crack growth behavior of a structural steel weldment was studied in room temperature ambient atmosphere. The investigation also examined the influence of the heat affected zone on the fatigue threshold and the fatigue crack growth rate. The influence of load ratio on the fatigue threshold and the fatigue crack growth rate was also studied. Micromechanism of crack growth process in the threshold region was also investigated. Compact tension specimens were prepared from ASTM grade A514 structural steel in such a way that the cracks propagated through the heat affected zone, base metal and weldment. Welding was done by the shielded metal arc welding (SMAW) process.

The results of the present investigation indicate that the fatigue crack growth rate was lower at all load ratios in the linear region when the crack propagated through the base metal. The fatigue threshold was highest in these specimens. The threshold was found to decrease with an increase in load ratio and a non-linear power law relationship was found to exist between the load ratio and the fatigue threshold. The crack growth process was found to be predominantly by striations. Extensive crack branching and secondary cracking were observed in high ΔK regions whereas crack branching was not generally observed in the threshold region.

INTRODUCTION

In recent years there has been significant interest in crack propagation and in fatigue threshold /1,2/. Design of structural components against fatigue failure on the basis of fatigue threshold has nowadays become an accepted practice. Fatigue threshold, ΔK_{th}, defines the stress intensity factor below which the pre-existing cracks or flaws present in a structural component will not propagate in cyclic loading situations (Fig. 1). Hence, structural components designed on the basis of fatigue threshold are expected to have infinite lives or at least last for a very long period of time.

Numerous variables /3-9/ can influence the fatigue crack growth rate and threshold parameter. Among these the influence of microstructure and load ratio are most important from a practical point of view. Even though in the past many studies /10-21/ have examined the influence of load ratio and microstructure on fatigue crack growth rate and fatigue threshold in a wide variety of materials, relatively little information is available on the influence of load ratio and microstructure on fatigue crack growth rate and the fatigue threshold in the case of structural steel weldments. The present investigation examined the influence of the heat affected zone as well as load ratio on the fatigue crack growth rate and fatigue threshold in a structural steel weldment of ASTM grade A514. The welding was done using the shielded metal arc welding process (SMAW).

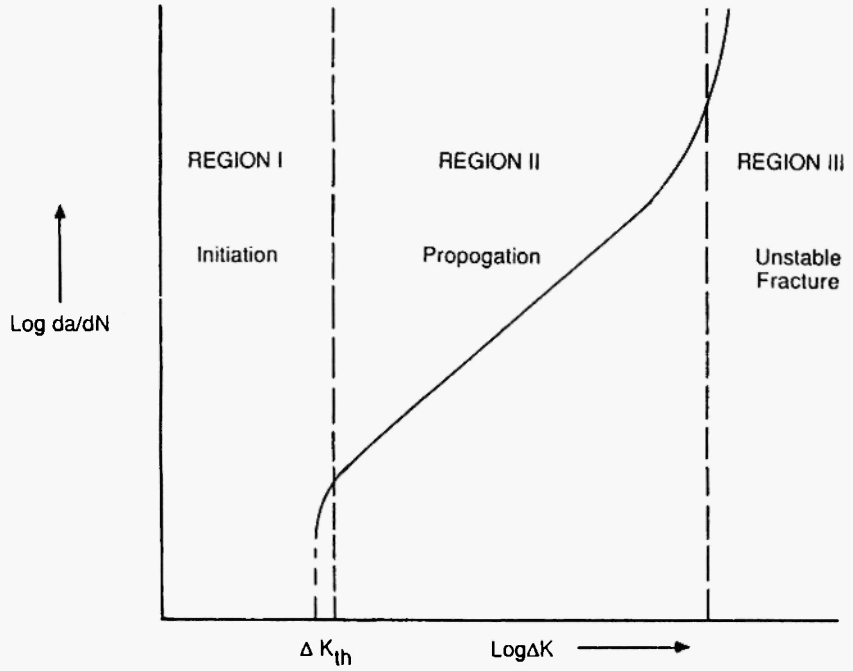

Fig. 1: Schematic representation of fatigue crack growth according to Paris equation.

EXPERIMENTAL PROCEDURE

Material

The material chosen for this investigation was structural steel ASTM grade A514. This material is used extensively in industrial steam generators as a forced and induced draft fan material where the temperature can be of the order of 100-200°F. In such applications, the material can undergo cyclic loading or fatigue fracture. Hence, fatigue crack growth rate data of this material are extremely important and needed for safe life prediction of these components.

Specimen Preparation

Two inch (50.8mm) wide compact tension specimens were prepared from ASTM grade A514 structural steel weldments. The specimens were designed in three different ways. In the first series of specimens (designated as the B1 series), the crack tip was located at the mid-section of the weld metal. In the second series of specimens (designated as the B2 series), the crack tip was located in such a way that the crack would propagate through the heat affected zone. In the third series of specimens (designated as the B3 series), the notch of the crack was oriented in such a way that the crack would propagate through the base metal. The welding for all these specimens was done using the shielded metal arc welding process (SMAW) as per American Welding Society standard AWS 14-6. A full penetration fusion welding process was employed. Table 1 shows the designation of the specimens. The chemical compositions of the weld deposit and the base metal are reported in Table 2.

Table 1

Specimen designations

B1:	Crack notch oriented through the weld metal.
B2:	Crack notch oriented through the heat affected zone.
B3:	Crack notch oriented through the base metal.

Table 2

Chemical analysis (weight percent)

	C	Mn	P	S	Si	Ni	Cr	Mo
Weld Deposit	0.18	1.02	0.008	0.015	0.60	0.13	0.65	0.25
Base Metal	0.1	1.20	0.020	0.030	0.55	----	----	----

The compact tension specimens used in this study were prepared as per ASTM standard E-647 /2/. The thickness of the specimens was about 6mm (0.25 inch) and width was 50.8mm (2 inch). The initial aspect ratio was kept at $\frac{a}{W}=0.30$. A schematic of the compact tension specimens used in this investigation is shown in Fig. 2.

Fatigue Testing

The specimens were ground on both surfaces and polished with 600 grit emery paper. This was found extremely useful in locating the crack tip during fatigue testing. The specimens were initially precracked in fatigue for 2 mm at a ΔK level of 15 MPa$\sqrt{m}$ to produce a sharp crack front. After fatigue precracking, fatigue testing was carried out in a servohydraulic MTS (Material Test System) test machine under load control mode. All testing was carried out in tension-tension mode in room temperature ambient atmosphere. A constant amplitude sinusoidal wave form was employed and tests were carried out at several load ratios (R) such as R = 0.1, 0.3, 0.5 and 0.9.

The crack lengths were monitored with the help of an optical traveling microscope. The crack lengths and number of cycles were measured continuously. The crack growth rate was determined as per ASTM standard E-647 /2/ test procedures.

The threshold was determined using the load shielding technique. The threshold was determined by slowly decreasing the load values and recording the crack growth rate. This reduction of load was at any stage done maximum up to 5% and that also only after the crack had grown by at least 1mm in the previous ΔK level. In this way, any retardation effect due to previous overload was avoided. The threshold was identified as the ΔK at which the crack growth rate was on the order of 10^{-10}m/cycle, as per ASTM standard E-647 /2/. At least 3 specimens from each series were tested and the average values from these specimens were taken as being the representative of the crack growth rate and fatigue threshold. To determine the influence of load ratio on the fatigue crack growth rate data and fatigue threshold, the fatigue testing was carried out at several load ratios such as R = 0.1, 0.3, 0.5 and 0.9, respectively.

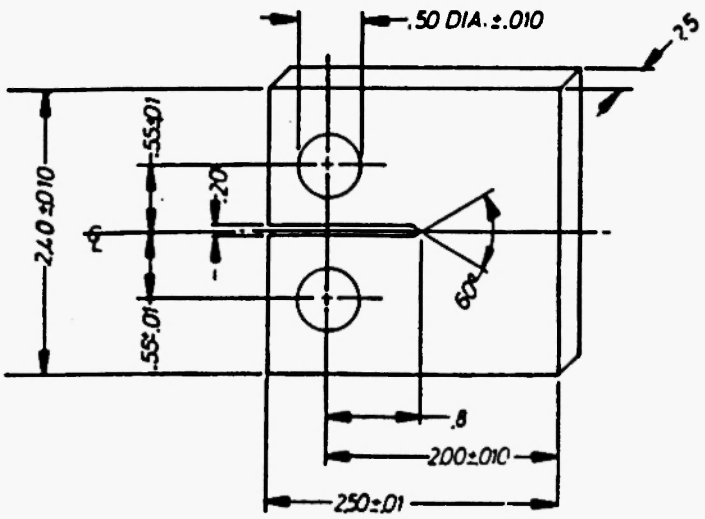

Fig. 2: Compact tension specimen:
Scale: Full size
All dims. in inches
Materials: ASTM Grade A514.

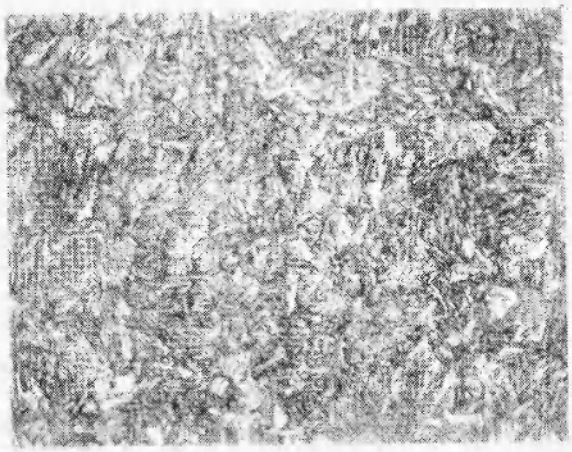

Fig. 3a: Microstructure of weld metal (B1), magnification 500x.

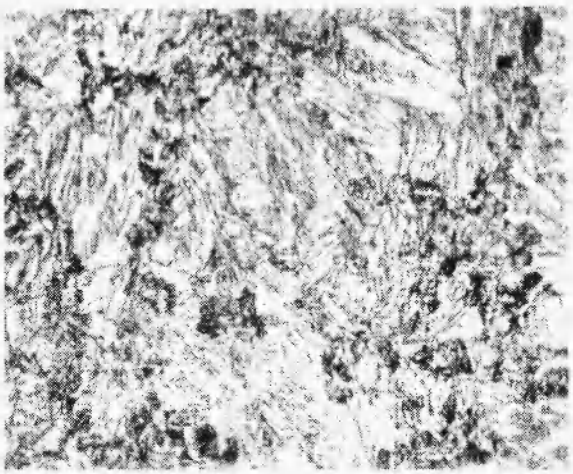

Fig. 3b: Microstructure of heat affected zone, magnification 500x.

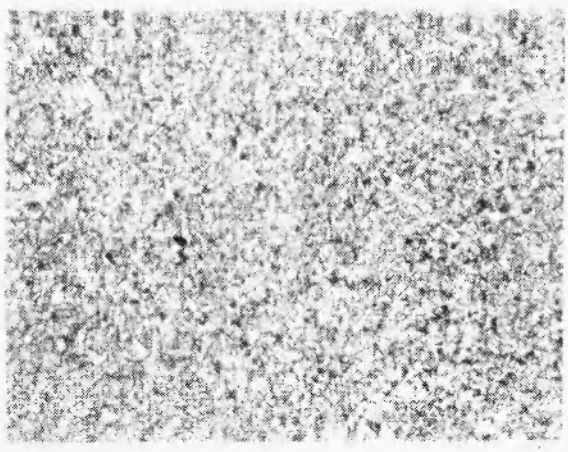

Fig. 3c: Microstructure of base metal (B3), magnification 500x.

Data Analysis

The data were analyzed using the Paris equation /1/ with the help of a computer program. A modified incremental polynomial technique was used to determine the fatigue crack growth rate /2/ $\left(\frac{da}{dN}\right)$ from the plot of crack length versus the number of cycles as per ASTM standard. The crack growth rate $\left(\frac{da}{dN}\right)$ and stress intensity range (ΔK) was then plotted on a log-log scale. The slope (m) and linear intercepts of the curves (C) were then determined for each series of specimens for each load ratio.

RESULTS AND DISCUSSION

Influence of Microstructure on Fatigue Crack Growth Rate

The microstructures of the materials in B1, B2 and B3 conditions are shown in Fig. 3a-c, respectively. The hardness values of the materials are reported in Table 3. The parent austenitic grain sizes were measured by an image analyzer on these specimens after etching. These measurements showed that B2 specimens had coarser grain sizes than either B1 or B3. The average prior austenitic grain diameter of B2 specimens was of the order of 52 μm compared to 40 μm for B1 and 22 μm for B3 specimens. Examination of steel weld metal and heat affected zone regions also revealed nonmetallic inclusions, pearlite colonies, and second phase regions (martensite and retained austenite). These inclusions often served as crack initiation sites

Table 3

Hardness of the materials

Specimen Series	Hardness Rockwell C
B1	23.5
B2	24
B3	27

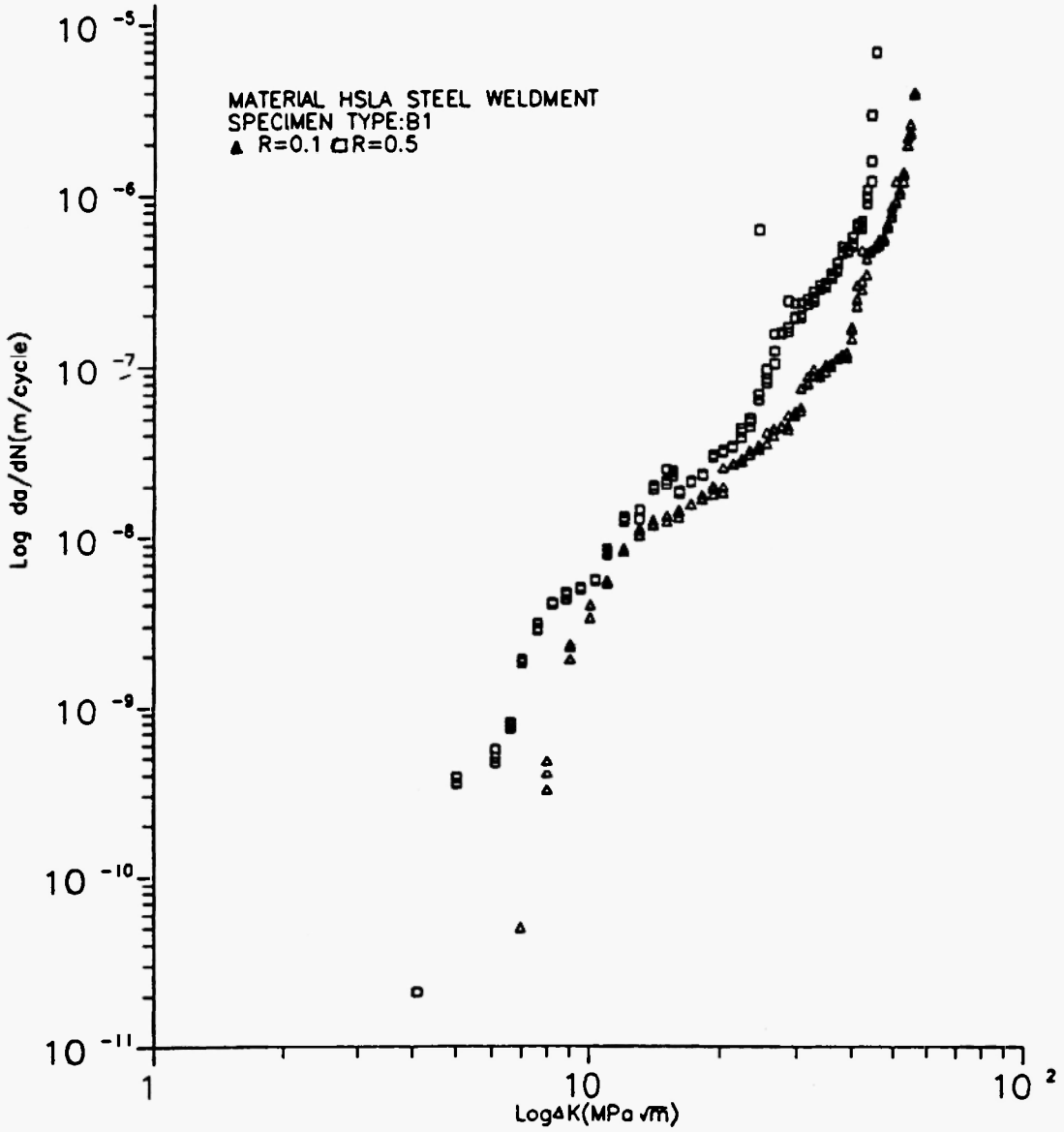

Fig. 4: Effect of load ratio on fatigue crack growth rate (B1).

for fatigue cracks and in most cases microcracks originated from these regions and joined with the main propagating crack.

Fig. 4 reports the fatigue crack growth rate data for B1 specimens at two different load ratios, R = 0.1 and R = 0.5. The fatigue crack growth rate at high load ratio (R = 0.5) was greater than at a load ratio of R = 0.10. Fig. 5 reports the fatigue crack growth rate data for B2 specimens at two different load ratios. In Fig. 6, the fatigue crack growth rate data for B3 specimens at four different load ratios (R = 0.1, R = 0.3, R = 0.5 and R = 0.9) are reported. All these figures indicate that the near threshold crack growth rate in these specimens generally increases with increase in load ratio. In Fig. 7, the crack growth rates of B1, B2 and B3 specimens are compared at the same load ratio, R = 0.1. In Fig. 8, the fatigue crack growth rate data of these B1, B2 and B3 specimens are compared at the same load ratio of R = 0.5.

Fig. 7 shows that the crack growth rate for the B3

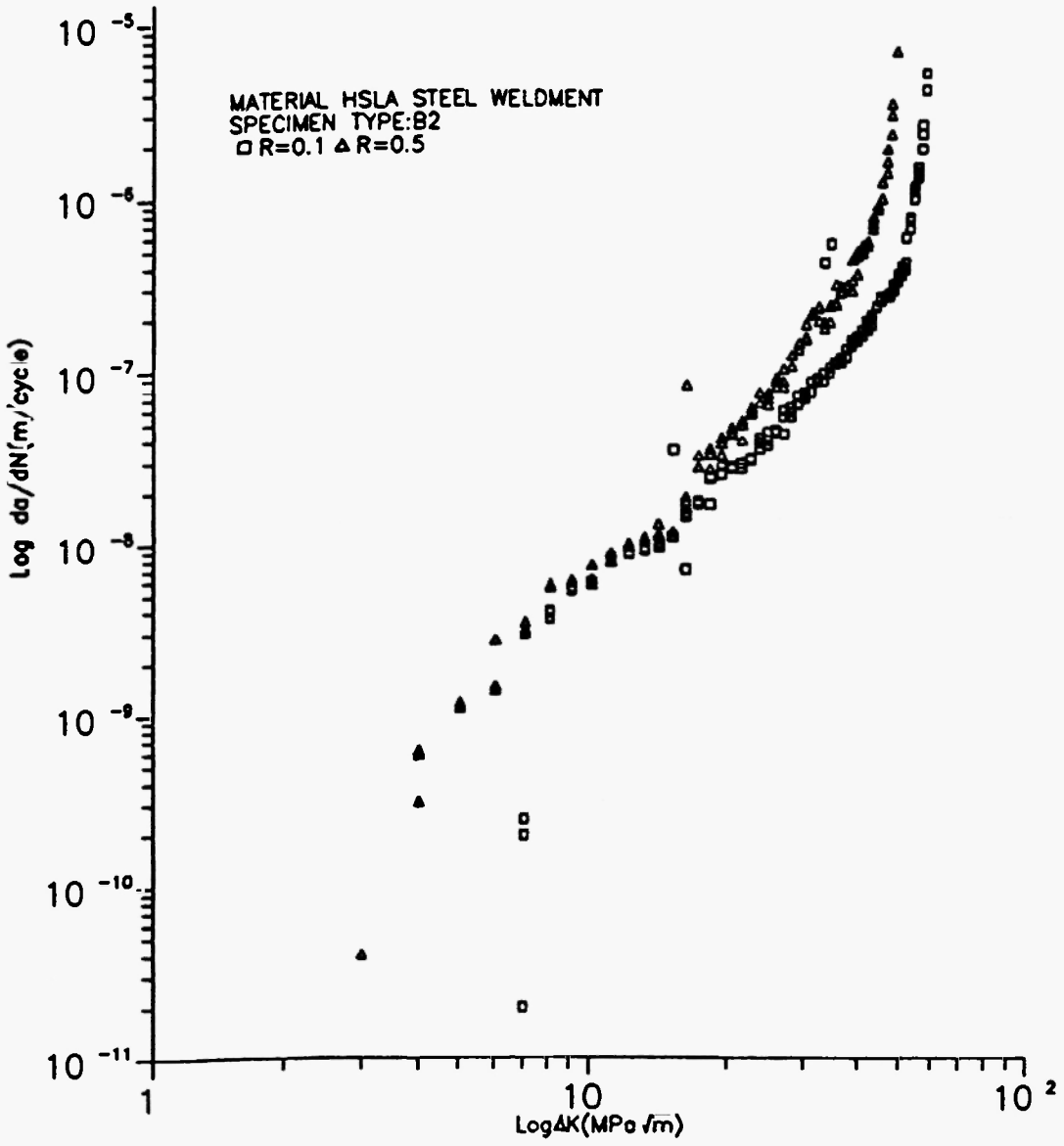

Fig. 5: Effect of load ratio on fatigue crack growth rate (B2).

specimen was lower in the threshold region as well as linear region than either the B1 or B2 specimens. As mentioned earlier, the B3 specimens are those where the crack propagated through the base metal. Hence, these results indicate that near-threshold crack growth rates are lower in the base material than in either HAZ (B2) or weld metal (B1). The data reported in Fig. 8 also show a similar trend, i.e., at the same load ratios, the near-threshold crack growth rate in the B3 specimen was lower than in either the HAZ or the weld metal. The crack growth rate in the very high ΔK region was higher for the B3 specimen at the load ratio of R = 0.5. Comparing the results of B1 and B3 specimens in these figures (7 and 8), it becomes obvious that weldment specimens (B1) have a higher crack growth rate than base metal (B3) specimens in the low ΔK region. The lower crack growth rate in B3 specimens in linear region is probably due to its smallest prior austenitic grain size.

Table 4 reports the fatigue threshold data for B1, B2

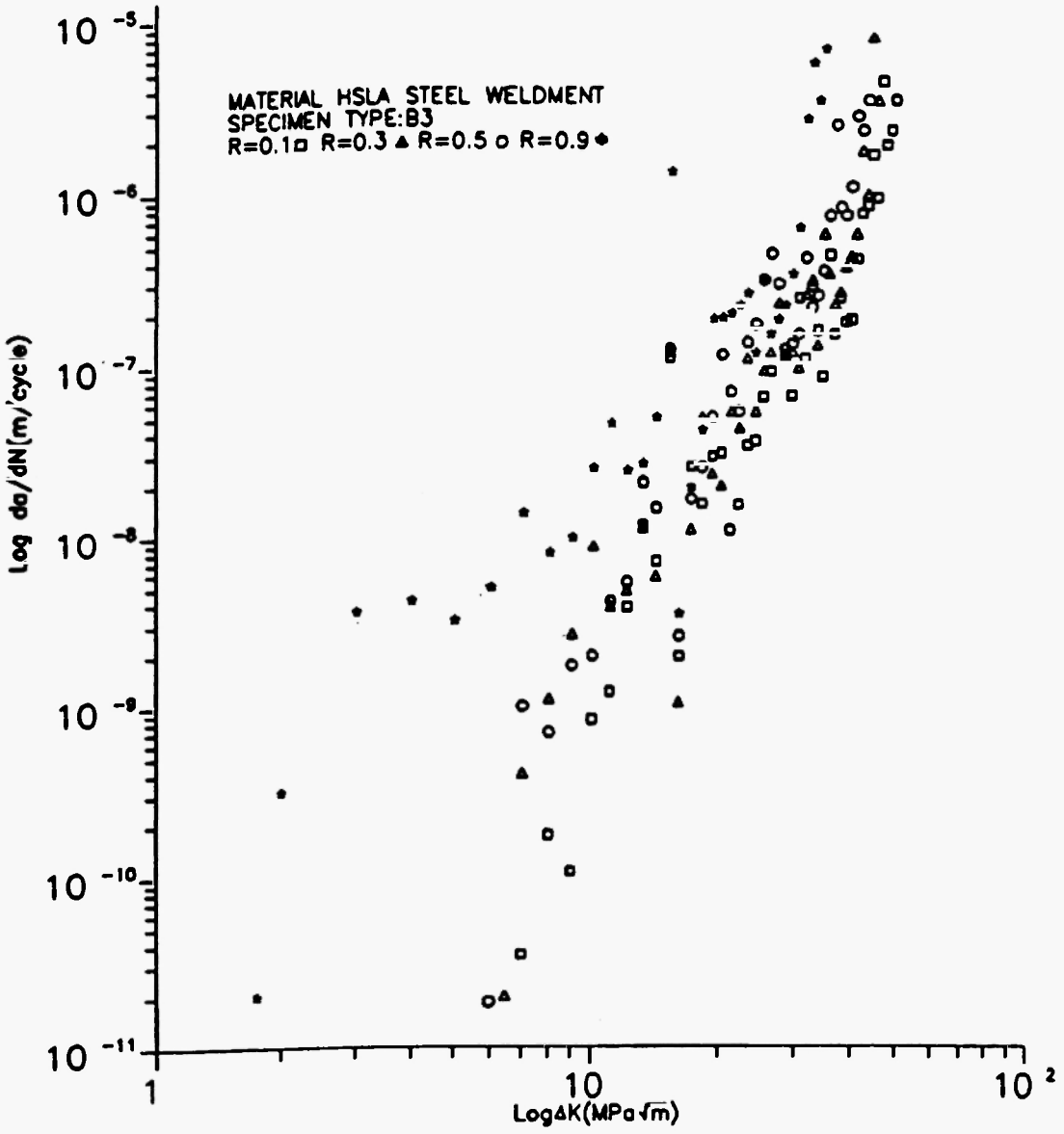

Fig. 6: Effect of load ratio on fatigue crack growth rate (B3).

and B3 specimens. In Table 5, the Paris constants, C and m, for B1, B2 and B3 specimens are reported for some of the load ratios. Generally, at the same load ratios (R = 0.3 and 0.5), the fatigue threshold, ΔK_{th}, is lower in B2 specimens than in either B1 or B3 specimens. At R = 0.1, the threshold values for all those specimens B1, B2 and B3 were very similar. The reason for this is not very clear yet. The higher near-threshold crack growth rate in B2 specimens (Fig. 8) has resulted in a lower fatigue threshold in these specimens. Interestingly, even though B1 and B2 specimens had similar hardnesses, the crack growth rate in the linear region in B2 specimens was higher.

B2 specimens had coarser grains compared to B1 and B3. Generally, fatigue threshold increases with increases in grain size /22/ as a result of significant increases in roughness-induced crack closure /23,24/. This crack closure effect will reduce the effective stress intensity factor ($\Delta K_{eff} \approx K_{max} - K_{op}$) and, hence, the mechanical driving force for propagation of a crack.

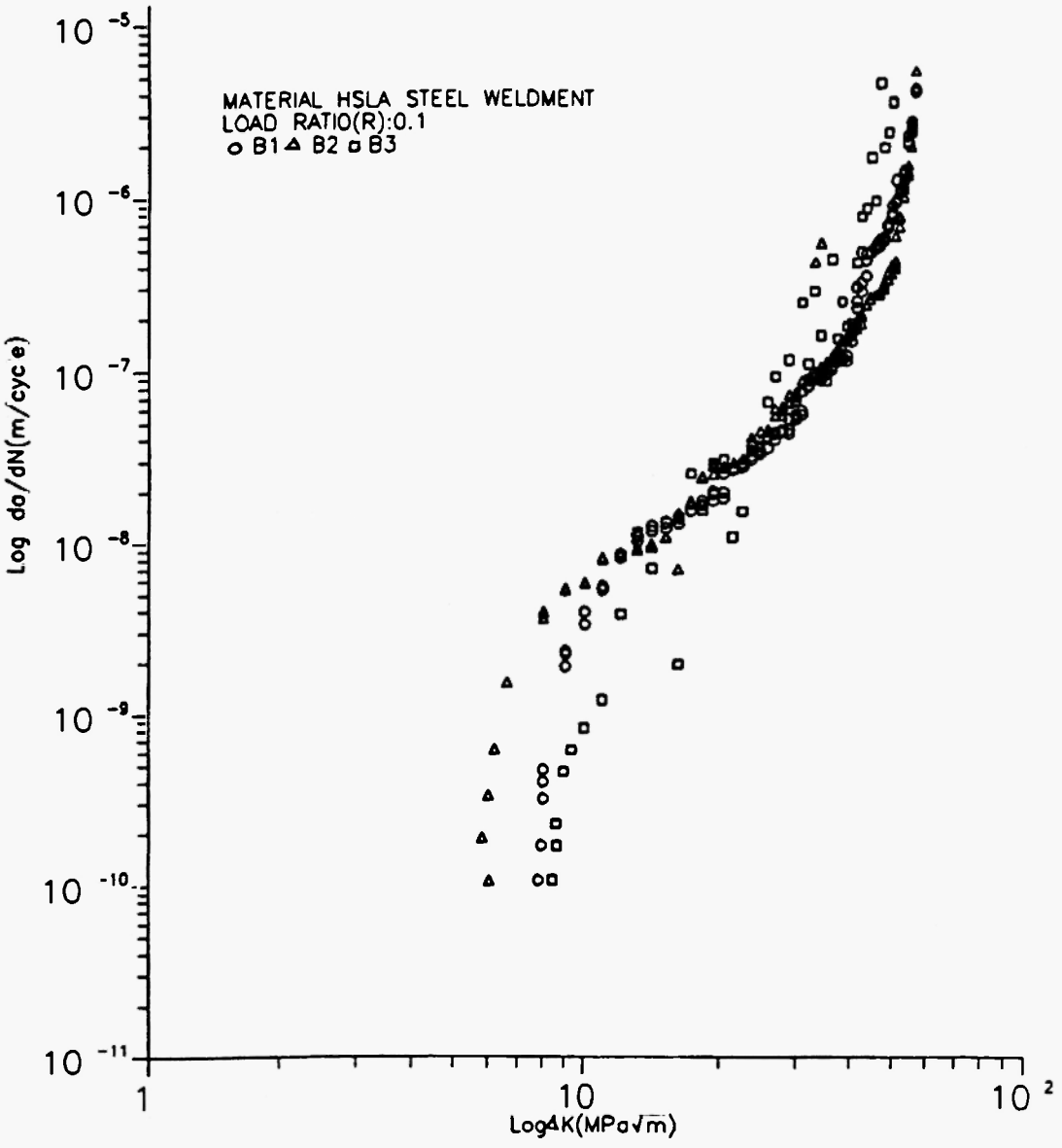

Fig. 7: Comparison of fatigue crack growth rates for B1, B2 and B3 specimens (R = 0.1).

Based on the above facts, one would expect a higher value of fatigue threshold and lower crack growth rate in B2 specimens. However, our test results indicate that the fatigue threshold is lower and the crack growth rate is higher in B2 specimens compared to B1 and B3. This is due to the fact that residual tensile stresses /25/ exist in the heat affected zones as a result of uneven cooling and heating processes during the welding cycle. This tensile residual stress in the HAZ would increase the mechanical driving force for crack propagation and consequently increase the crack growth rate and, therefore, reduce the fatigue threshold in B2 specimens. This effect becomes significantly higher as higher load ratio and crack driving force become higher, thus increasing the crack growth rate.

In the range of ΔK from about 8 to 20 Mpa$\sqrt{m}$, there appears to be no significant effect of load ratio on crack growth rate in B2 specimens (see Fig. 5). However, below a ΔK level of 8 Mpa$\sqrt{m}$ and above 20 Mpa$\sqrt{m}$ one can clearly see a significant increase in

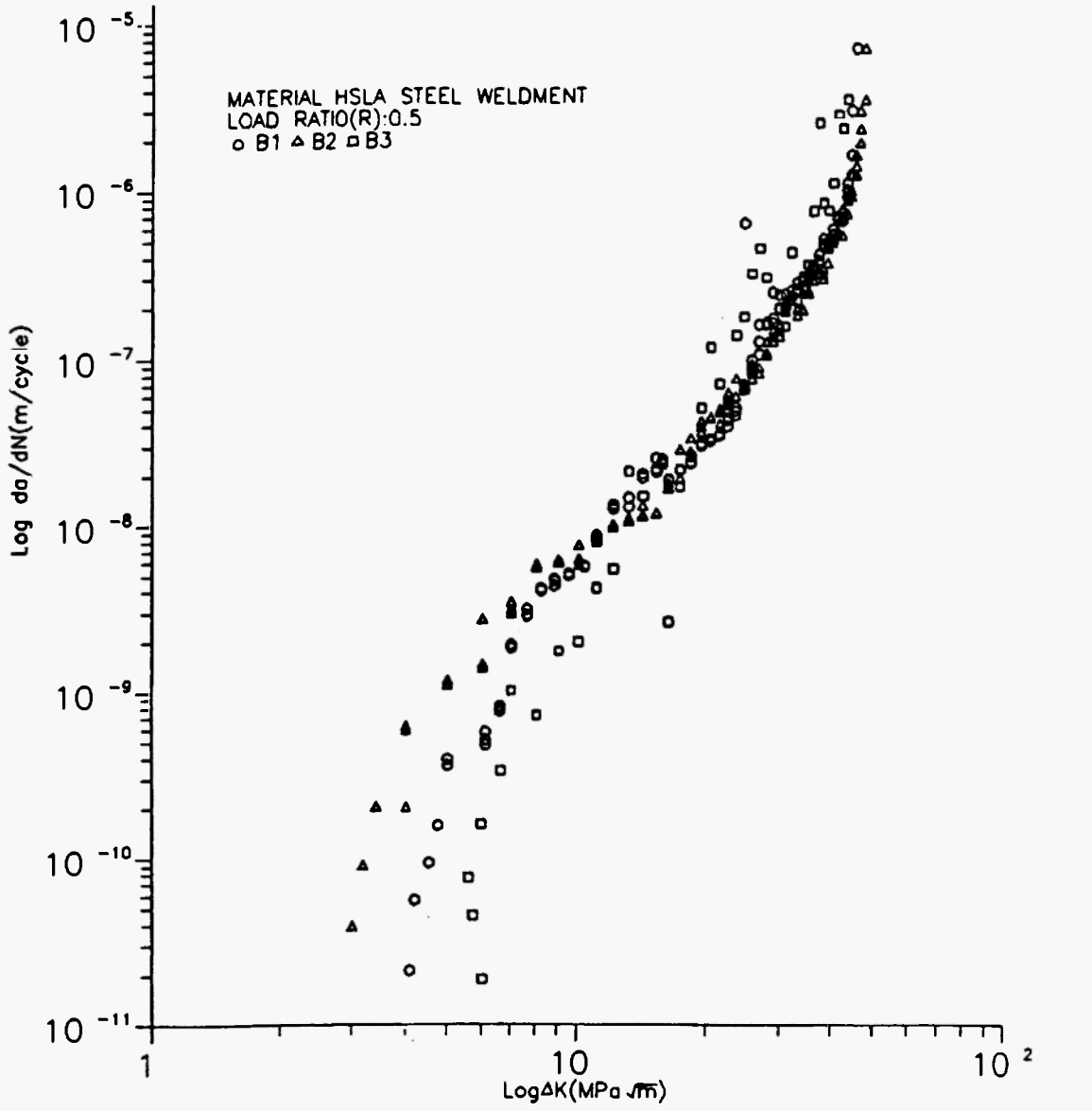

Fig. 8: Comparison of fatigue crack growth rates for B1, B2 and B3 specimens (R = 0.5).

crack growth rate at higher load ratios. This behavior was unique for B2 specimens since similar behavior was not observed in B1 and B3 specimens. The reason for this behavior is not clear. Further studies are needed to resolve this issue. However, it appears that in this ΔK range, the decrease in effective stress intensity factor due to roughness-induced crack closure compensates for any increase in effective stress intensity range at a higher load ratio. This behavior may be explained by the fact that roughness-induced crack closure can also occur at high load ratios /21/.

Influence of Load Ratio on Fatigue Threshold

Fig. 9 presents a plot of ΔK_{th} versus load ratio R for B3 specimens. One can clearly observe that fatigue threshold decreases with load ratio (R) in these specimens and there appears to exist a non-linear power law relationship between fatigue threshold ΔK_{th} and load ratio (R).

Table 4

Fatigue threshold of the materials

Specimen Series	Load Ratio	K_{th} MPa√m
B1	0.1	7.50
B1	0.3	5.80
B1	0.5	4.10
B1	0.9	1.70
B2	0.1	7.0
B2	0.3	5.1
B2	0.5	3.0
B2	0.9	1.35
B3	0.1	6.74
B3	0.3	6.5
B3	0.5	6.0
B3	0.9	1.80

Table 5

Paris constants

Specimen series	Load ratio (Rc)	Paris constants C	m
B1	0.1	1.05×10^{-11}	2.5579
B1	0.5	8.42×10^{-14}	4.2971
B2	0.1	1.25×10^{-11}	2.57
B2	0.5	2.01×10^{-12}	3.3325
B3	0.1	8.72×10^{-14}	4.1343
B3	0.5	2.12×10^{-13}	4.2125
B3	0.9	6.5×10^{-11}	2.4341

Vosikovsky /16/ analyzed data from the literature concerning the effect of load ratio on fatigue threshold and found that the threshold decreases in most cases with an increase in load ratio. He proposed an empirical relationship, $\Delta K_{th} = \Delta K_{th0}(1\text{-}bR)$, where ΔK_{th0} is the value of the threshold at a load ratio R = 0 and b is a constant dependent upon material. Based on similar observations, Barsom /26/ proposed a relationship of the nature, $\Delta K_{th} = \Delta K_{th0} - BR$, where B is an environment dependent constant. Klensil and Lucas /27/, on the other hand, observed a nonlinear power low relationship between fatigue threshold and load ratio and proposed a relationship, $\Delta K_{th} = \Delta K_{th0}(1\text{-}R)^{\gamma}$, where γ is a material environment dependent constant. Our test results show that there is a non-linear power law relationship between the load ratio and fatigue threshold in these materials.

Fractography

The SEM fractographs of B1, B2 and B3 specimens in the threshold region are shown in Figs. 10a-c. The fractographs in the high ΔK region for B1, B2 and B3 specimens are shown in Figs. 11a-c.

The fractographs indicate that the fatigue crack growth mechanism is mainly by ductile striations in B3 specimens in both threshold and high ΔK regions. Whereas in the high ΔK region there was extensive crack branching, in the threshold region the crack branchings were very few. On the other hand, the fracture surface shows faceted fracture surface in the threshold region for B2 specimens, but in the high ΔK region the crack growth process appears to be by ductile striations. In the case of weld metals (B1), the crack growth mechanism in the threshold region appears to be a mixture of microvoids and ductile striations. However, in the high ΔK region the crack growth process appears to be exclusively by ductile striations. Thus there is a change in crack growth mechanisms in B1 and B2 specimens from the low ΔK to the high ΔK regions.

CONCLUSIONS

1. The near-threshold fatigue crack growth rate was found to be lower in B3 specimens where the fatigue

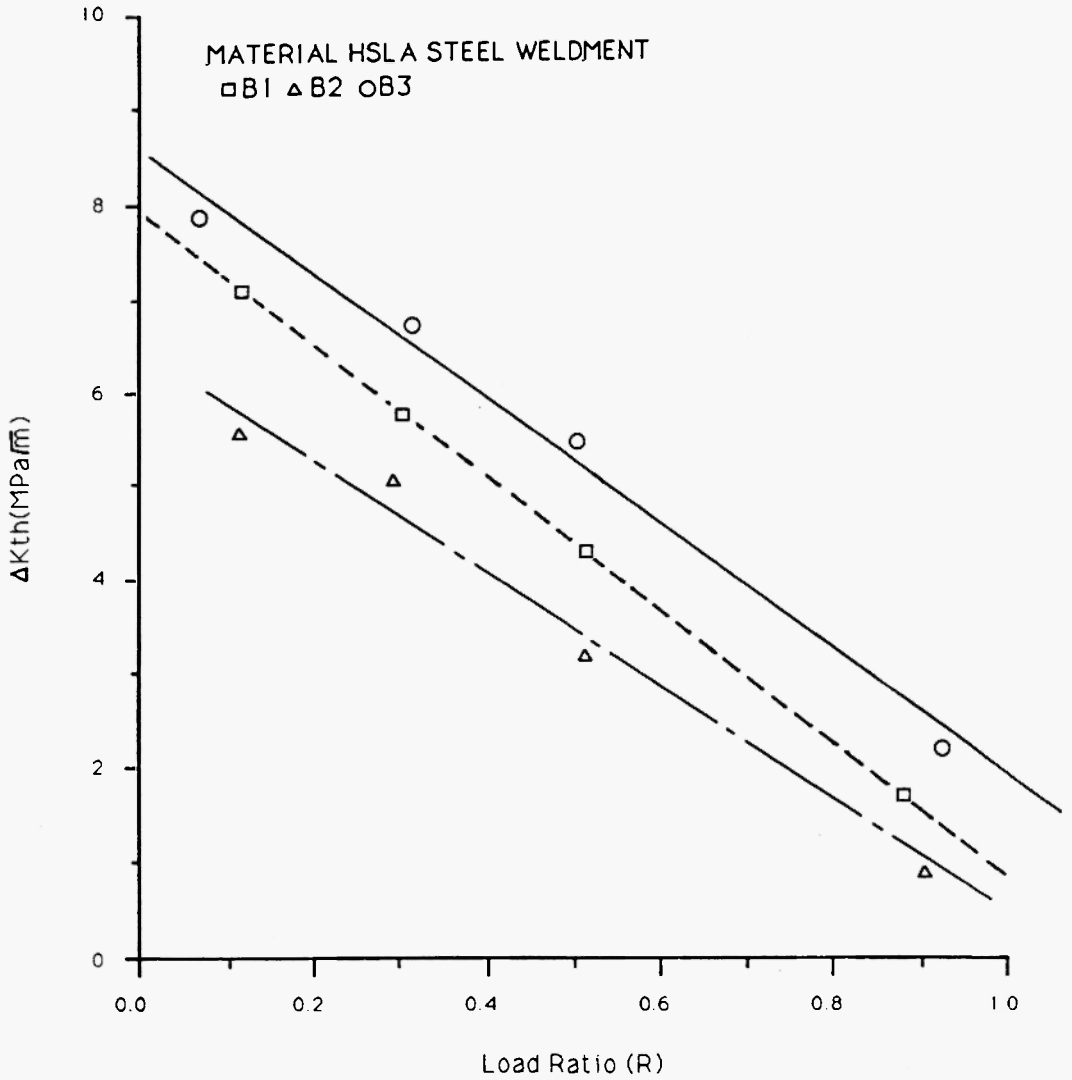

Fig. 9: Effect of load ratio on fatigue threshold.

crack propagated through the base metal.

2. Generally at the same load ratios, the fatigue threshold for B3 specimens was higher than for either the B1 or B2 specimens.

3. The fatigue threshold was found to decrease with an increase in load ratio in all these specimens and a non-linear power law relationship was found to exist between ΔK_{th} and the load ratio for all these materials.

4. Load ratio had a significant effect on the crack growth rate in the threshold region and in the very high ΔK region for the B2 specimens. However, in the intermediate range of ΔK, i.e. from 8 to 20 MPa$\sqrt{m}$, the load ratio did not have a significant influence on the crack growth rate for the B2 specimens.

5. Fatigue crack growth rate of the base metal was found to be lower than weldment and heat affected zone material in the linear region.

Fig. 10a: SEM fractograph of B1 specimens (weld metal) in threshold region).

Fig. 10b: SEM fractograph of B2 specimens (HAZ material) in threshold region.

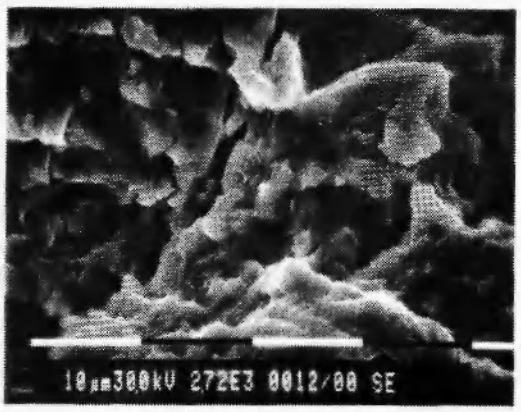

Fig. 10 c: SEM fractograph of B3 specimens (base metal) in threshold region.

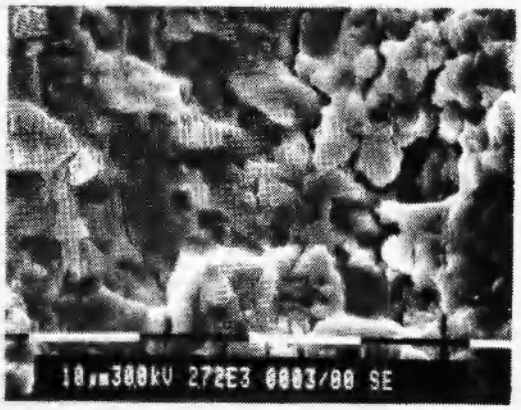

Fig. 11a: SEM fractograph of B1 specimens (weld metal) in high ΔK region.

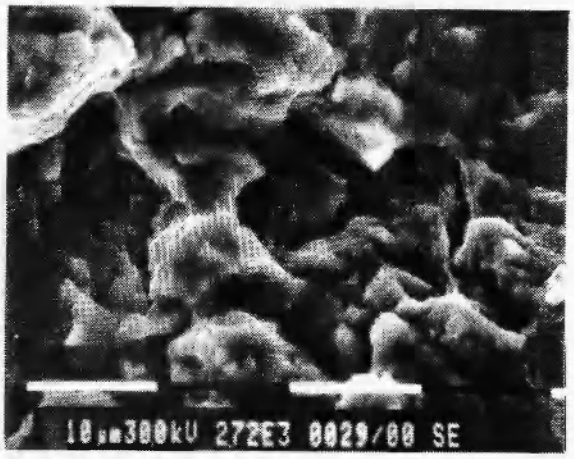

Fig. 11b: SEM fractograph of B2 specimens (HAZ material) in high ΔK region.

Fig. 11c: SEM fractograph of B3 specimens (base metal) in high ΔK region.

REFERENCES

1. Paris, P.C. and Erdogan, F., "A critical analysis of crack propagation law", *Journal of Basic Engineering*, 85(4), 528-538 (1963).
2. ASTM E-647, "Standard Test Method for Constant Load-Amplitude Fatigue Crack Growth Rates Above 10-8 m/cycle", Annual Book of ASTM, Standards, Vol. 03.01, 711-731 (1984).
3. Irving, P.R. and McCartney, L.N., "Prediction of fatigue crack growth rates: Theory, mechanisms, and experimental results", *Metal Science*, 11, 351-361 (1970).
4. Throop, J.F. and Miller, G.A., "Optimum Fatigue Crack Resistance", ASTM, Special Technical Publication No. 467, 154-168 (1970).
5. Putatunda, S.K., "Fracture toughness and fatigue crack growth rate", *Transactions of the Indian Institute of Metals*, 40, 34-38 (1987).
6. Lindley, T.C., Richards, C.E. and Ritchie, R.O., "The Mechanics and Mechanisms of Fatigue Crack Growth in Metals", Conference on Mechanics and Physics of Fracture, Cambridge Metal Society, London, 1, 238-248 (1975).
7. Benson, J.P. and Edmonds, D.V., "Microstructural effects on fatigue at intermediate and high crack growth rates in low alloy steel", *Materials Science & Engineering*, 38, 179-186 (1979).
8. Benson, J.P., "Influence of grain size and yield strength on threshold fatigue behavior of low-alloy steel", *Materials Science & Engineering*, 9, 535-539 (1970).
9. Drowse, K.R. and Richards, C.E., "Fatigue crack propagation through weld heat affected zones", *Metallurgical Transactions*, 2, 599-602 (1971).
10. Yu, M.T. and Topper, T.H.,"The effects of material strength, stress ratio, and compressive overload on the threshold behavior of a SAE1045 steel", *Journal of Engineering Materials*, 107, 19-26 (1977).
11. Clark, G. and Knott, J.F., "Effects of notches and surface hardening on the early growth of fatigue cracks", *Metal Science*, 11, 345-350 (1977).
12. Ritchie, R.O., "Near-threshold fatigue crack propagation in ultra-high strength steel: Influence of load ratio and cyclic strength", *Journal of Engineering Materials and Technology*, 96, 195-204 (1977).
13. Beevers, C.J., "Fatigue crack growth characteristics at load stress intensities of metals and alloys", *Metal Science*, 11, 362-367 (1977).
14. Kunio, T. and Yamada, K., "Microstructural aspects of the threshold condition for non-propagating fatigue cracks in martensitic-ferritic structures", presented at the ASTM NBS-NFS Symposium on Fatigue Mechanisms, Kansas City, MO, May 22-24, 1978: 1, 23-26 (1978).
15. Cooke, R.J., Irving, P.E., Booth, G.S. and Beevers, C.J., "Slow fatigue crack growth and threshold behavior of a medium carbon alloy steel in air and vacuum", *Engineering Fracture Mechanics*, 7, 69-77 (1975).
16. Vosikovsky, O., "Effect of stress ratio on fatigue crack growth rates in steels", *Engineering Fracture Mechanics*, 11, 595-620 (1979).
17. Barsom, J.M., "Fatigue behavior of pressure-vessel steels", *W.R.C. Bulletin*, 194, 113-124 (1974).
18. Yu, M.T., Hooper, T.H. and Au, P., "Effect of yield strength on fatigue threshold in low alloy steels", Second International Conference on Fatigue Thresholds, Birmingham, U.K., Sept. 3-7. 1984: 1: 20-28 (1984).
19. Ritchie, R.O., "Influence of microstructure on near-threshold fatigue crack propagation in ultra-high strength steels", *Metal Science*, 11, 368-381 (1977).
20. Cooke, R.J. and Beevers, C.J., "Slow fatigue crack propagation in pearlitic steels", *Materials Science and Engineering*, 13, 201-212 (1974).
21. Liaw, P.K. and Logdon, W.A., "The influence of load ratio and temperature on the near-threshold fatigue crack growth rate properties of pressure vessel steels", *Journal of Engineering Materials and Technology*, 107, 26-33 (1985).
22. Masounave, J. and Bailon, J.P., "Effect of grain size on the threshold stress intensity factor in fatigue of a ferritic steel", *Scripta Metallurgica*, 10, 165-173 (1976).
23. Elber, W., "Fatigue crack closure under cyclic tension", *Engineering Fracture Mechanics*, 2(1), 37-45 (1970).
24. Suresh, S. and Ritchie, R.O., "Near threshold

fatigue crack propagation. A perspective on the role of crack closure in fatigue threshold concepts", in: *Fatigue Threshold*, Davidson, D. and Suresh, S., eds., AIME, 227-261 (1984).

25. Easterling, K., "Introduction to Physical Metallurgy of Welding", Butterworths, 104-136 (1983).
26. Barsom, J.M., "Fatigue behavior of pressure vessel steels", *W.R.C. Bulletin*, **194**, 113-124 (1974).
27. Klensil, M. and Lukas, P., "Effect of stress cycle asymmetry on fatigue crack growth", *Materials Science & Engineering*, **9**, 231-236 (1972).